International Journal of Scientific Research & Engineering Trends
Volume 9, Issue 4, Jul-Aug-2023, ISSN (Online): 2395-566X

Cfd Analysis Of Flat Plate Solar Collecter

M.Tech. Scholar Arjun Kumar Prajapati, Prof. Brijendra Kumar Yadav
Department of Mechanical Engineering,
PCST Bhopal,MP,India

Abstract- Fossil fuel sources are confined and so the present scenario of energy consumption and growth are not sustainable in the longer term. The energy demand for different applications can be attained by pick up of the solar energy efficiently. Solar energy is the most promising source of energy and the simplest and efficient way of using solar energy is to convert it into thermal energy for heating applications such as space heating, drying of agricultural products and various industrial applications by using solar air heater. The solar air heater is not efficient due to low convective heat transfer coefficient between absorber plate and flowing air. The low rate of heat transfer coefficient is due to presence of a viscous sub-layer. Turbulence element on absorber plate breaks up the laminar sub-layer and increases heat transfer. Increased heat transfer makes the system more effective. Various investigators have investigated the effect of heat transfer and friction factor in various geometries of artificial roughness in a solar air heater duct.

Keywords- Solar flat plate collector, energy consumption, absorber plate, performance

I. INTRODUCTION

Fossil fuel sources are confined and so the present scenario of energy consumption and growth are not sustainable in the longer term [1]. The energy demand for different applications can be attained by pick up of the solar energy efficiently. Solar energy is the most promising source of energy and the simplest and efficient way of using solar energy is to convert it into thermal energy for heating applications such as space heating, drying of agricultural products and various industrial applications by using solar air heater. The solar air heater is not efficient due to low convective heat transfer coefficient between absorber plate and flowing air. The low rate of heat transfer coefficient is due to presence of a viscous sub-layer. Turbulence element on absorber plate breaks up the laminar sub-layer and increases heat transfer. Increased heat transfer makes the system more effective. Various investigators have investigated the effect of heat transfer and friction factor in various geometries of artificial rough- ness in a solar air heater duct.

Solar air heaters are simple in design and construction. They are widely used as collection devices having applications such as space heating and crop drying. Efficiency of flat plate solar air heater is low because of low convective heat transfer coefficient between absorber plate and flowing air that increases absorber plate temperature, leading to higher heat losses to environment. Low value of heat transfer coefficient is due to presence of laminar sub- layer that can be broken by providing artificial roughness on heat transferring surface [1]. Efforts for enhancing heat transfer have been directed toward artificially destroying or disturbing this laminar sub-layer. Artificial roughness in form of ribs and in various configurations has been used to create turbulence near wall or to break laminar sub-layer. Artificial roughness results in high frictional losses leading to more power requirement for fluid flow. Hence turbulence has to be created in region very close to heat-transferring surface for breaking viscous sub-layer. Core fluid flow should not be unduly disturbed to limit increase in pumping requirement. This is done by keeping height of roughness elements small in comparison to duct dimensions [2].

Solar energy is one of the most useful renewable energy resources without any adverse effects on the environment.

Solar energy is widely used for generating electricity, heating and various industrial applications. Solar air heaters (SAHs) are simple in design and generally used as solar thermal collectors [1]. SAHs are inexpensive and the most widely used collection devices because of their inherent simplicity. SAHs form the foremost component of a solar energy utilization system [2]. Figure 1 shows various components of a solar air heater. These air heaters absorb the irradiance and exchange it into thermal energy at the absorbing surface and then transfer this energy to a fluid flowing through the collector. An absorber plate is usually a thin metal sheet coated with an absorbing substance such as black or selective coating to absorb solar radiations. The glazing provides a rigid, protective structure for the entire collector assembly. Insulation beneath the absorber and fluid flow passages inhibits downward heat loss. SAHs are found in several solar energy applications, especially for space heating, timber seasoning and agriculture drying [3].

International Journal of Scientific Research & Engineering Trends
Volume 9, Issue 4, Jul-Aug-2023, ISSN (Online): 2395-566X

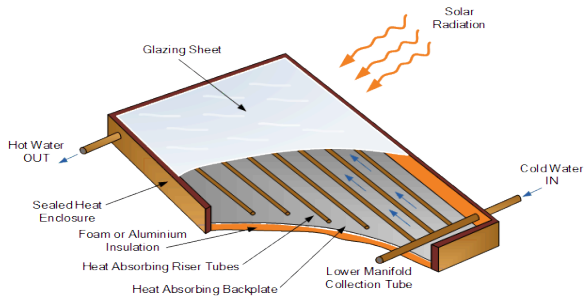

Fig. 1: Schematic of a simple solar air heater.

Conventional SAH has poor thermal performance due to low convective heat transfer rate fromthe heated plate to the air. The use of rib roughness on the heated plate is one of the heat transferaugmentation methods employed in SAH systems. The idea of artificial roughness was initiallyapplied to compact heat exchangers and cooling of gas turbine blades and electronic equipment [4].Motivated by the improvements in thermal performance through the application of rib roughnessin various configurations for gas turbine blade cooling, many researchers tried different roughnessgeometries to study their effect on the heat transfer of solar collectors and reported improvement inthermal performance [4–14]. Several experimental studies in SAH performance had been conducted tooptimize the roughness elements of shape, size, orientation relative to flow direction [5]. This study presents CFD analysis on the thermal hydraulic characteristics of a three-dimensional SAH channel with square-sectioned discrete multi-V-pattern rib roughness. Average Nusseltnumber, friction factor and thermal hydraulic performance parameter were reported as functions ofReynolds numbers.

II. RESEARCH METHODOLOGY

Problem Formulation

In this study, various turbulence-inducing elements in a straight-shaped pipe were investigated numerically. First, the impact of different turbulent inducing elements geometry was evaluated for this type of collector, then with using the case that had the highest heat transfer, the effect of two hybrid nanofluids and pure water was studied. In the third stage, the fluid with the highest heat transfer was investigated at various concentrations, and connected results, including Friction factor and Heat transfer coefficient, were compared in the diagrams. The outcomes of this study can be used to enhance the efficiency of FPSCs, which are among the pioneers in the field of renewable energy today.

Computational domain

Flat plate solar collectors have a larger scale than the paper in the study. Because this study aims to examine heat transfer changesusing different turbulence-inducing elements, the problem must be solved in 3D, and its mesh size must be small enough to show theeffect of the secondary flows.

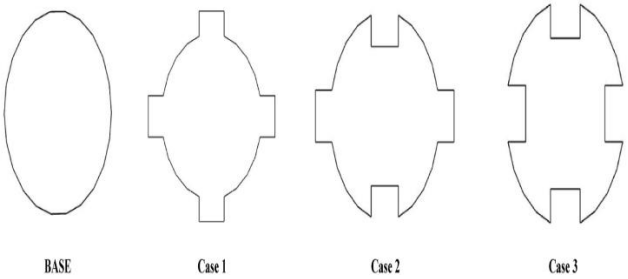

Fig. 2. The geometry of base pipe and various turbulent-inducing elements (Nabi et al. 2022)

Table 1: The specifications related to the FPSC size(Nabi et al. 2022)

Specification	Value
Width of the plate	300 mm
Length of the plate	300 mm
Height of the turbulent-inducing elements	0.3 mm
The thickness of the turbulent-inducing elements	0.5 mm
Diameter of the base pipe	2 mm

The dimensions of the collector under study are 300 × 300 × 1.30 mm^3.Fig. 3.1 demonstrates the different shapes of Turbulent-inducing elements and base pipe in this study. The characteristics of the geometry are given in Table 1.

Governing differential equations

Continuity equation

$$\frac{\partial}{\partial x_i}(\rho u_i) = 0 \qquad (3.1)$$

Momentum Equation

$$\frac{\partial}{\partial x_i}(\rho u_i u_j) = -\frac{\partial P}{\partial x_i} + \frac{\partial}{\partial x_j}\left[\mu\left(\frac{\partial u_i}{\partial x_j} + \frac{\partial u_j}{\partial x_i}\right)\right] + \frac{\partial}{\partial x_j}\left(-\rho\overline{u_i' u_j'}\right) \qquad (3.2)$$

Energy equation

$$\frac{\partial}{\partial x_i}(\rho u_i T) = \frac{\partial}{\partial x_j}\left[(\Gamma + \Gamma_t)\frac{\partial T}{\partial x_j}\right] \qquad (3.3)$$

Boundary Condition

The initial temperature of the working fluid is 300 K. Top of the plate is exposed to a constant heat flux of 1000 W/m^2 . Side partsand the bottom of the solar collector are considered insulated. The boundary conditions were considered velocity inlet and pressureoutlet for inlet and outlet sections.

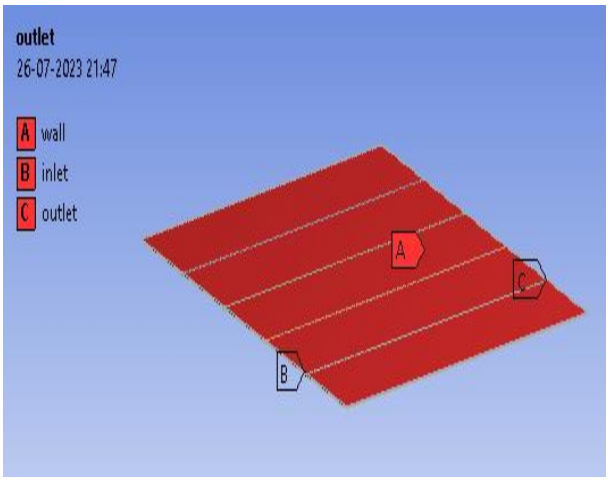

Fig. 3: Boundary condition for CFD analysis

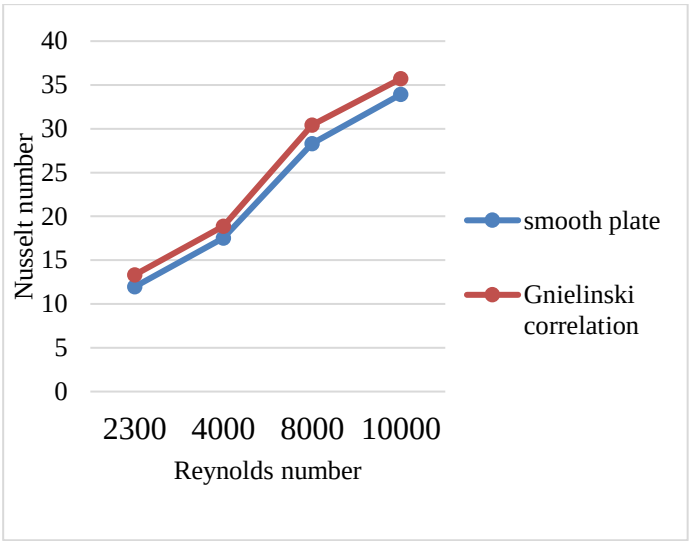

Fig. 4: Nusselt number validation

CFD Modelling

Commercially available ANSYS FLUENT v 15.0 was the CFD software employed to solve the concerned general differential equations numerically. This software numerically simulates using finite element method.

Set up and flow specification

The generated mesh was then exported to FLUENT where the different flow and physical properties were specified. The appropriate turbulent model was selected and the energy option was switched on. The working fluid was air and aluminum, because of its higher absorptivity, was the absorber plate. Their thermo-physical properties are mentioned in Table 2.

Table 2: Thermo-physical properties of working fluid

Parameter	Value
Density	1003.13 Kg/m^3
Specific heat	4127.99 j/kg-K
Thermal conductivity	0.6164 w/m-k
Viscosity	0.00105 kg/ms

III. RESULTS AND DISCUSSION

Model Validation

Figs. 4.1 show comparison of simulation values andthose predicted by Gnielinskicorrelation for Nusselt number.Absolute percentage deviation between predicted and simulationresults has been found to be 5% for Nusselt number. Excellent agreement between simulation andpredicted values establishes accuracy of measurement on CFD domain.The Gnielinskicorrelation for Nusselt number is given by

$$Nu = \frac{\left(\frac{f}{8}\right)(Re_{Dh}-1000)Pr}{1+12.7(f/8)^{\frac{1}{2}}(Pr^{\frac{2}{3}}-1)} \qquad (4.1)$$

Figs. 4 show comparison of simulation values andthose predicted by Gnielinskicorrelation for Nusselt number.Absolute percentage deviation between predicted and experimentalresults has been found to be 5% for Nusselt number. Excellent agreement between simulation andpredicted values establishes accuracy of measurement on CFD domain.

Temperature Profile

Much research is currently being done to increase the heat transfer rate in flat plate solar collectors. An easy and cheap way to improve heat transfer rate in heat exchangers without utilizing external power is turbulence-inducing elements. In the first part, the shape of turbulent-inducing elements under the heat flux of 1000 W/m^2 was evaluated. Fig. 4.2 shows the various cases under study, including the base model and various turbulent–inducing elements used to add rotational flow.

Fig. 4, a slice of the flat plate solar collector, shows how the temperature is distributed in the whole collector. As seen in the third case, the turbulence-inducing elements cause more circulating flow, disturb the thermal boundary layer, and have a better heat transfer. The temperature on the collector is high in BASE Model because it cannot transfer this heat to the tube, whereas the third case, which has a better heat transfer rate, has a colder collector temperature because due to better heat transfer, the inlet heat is transferred to the fluid and increases the outlet temperature.

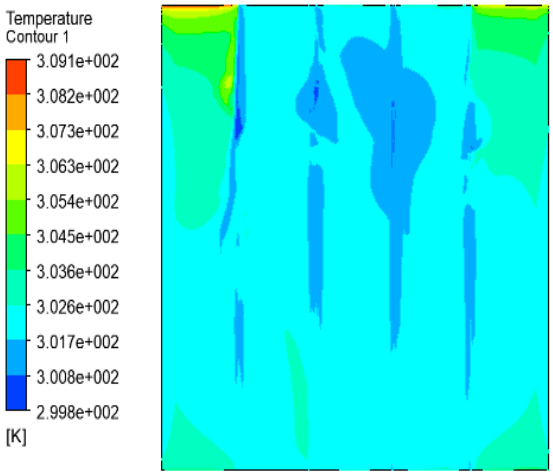

Smooth tube at Re= 2300

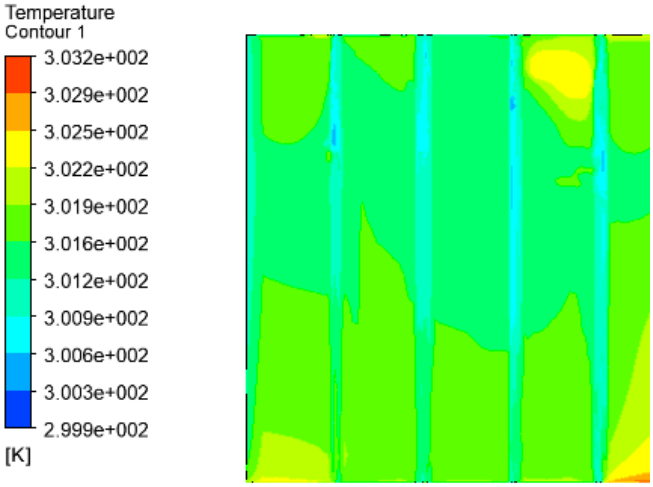

Smooth tube at Re= 4000

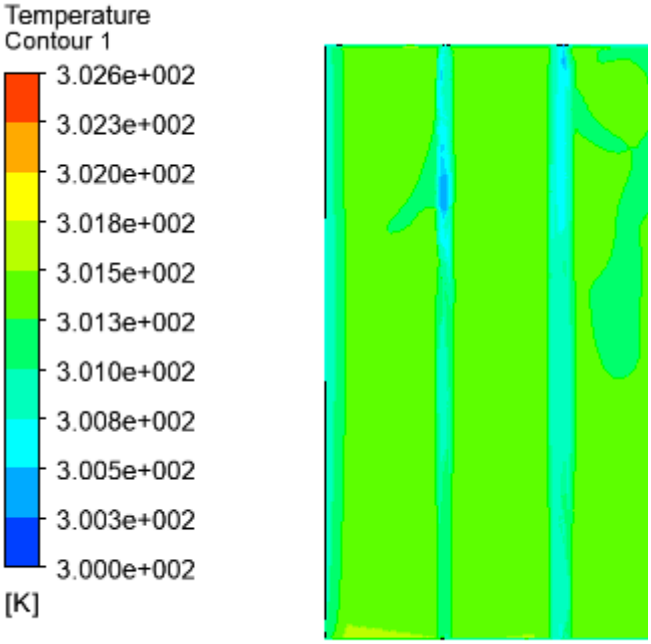

Smooth tube at Re= 8000

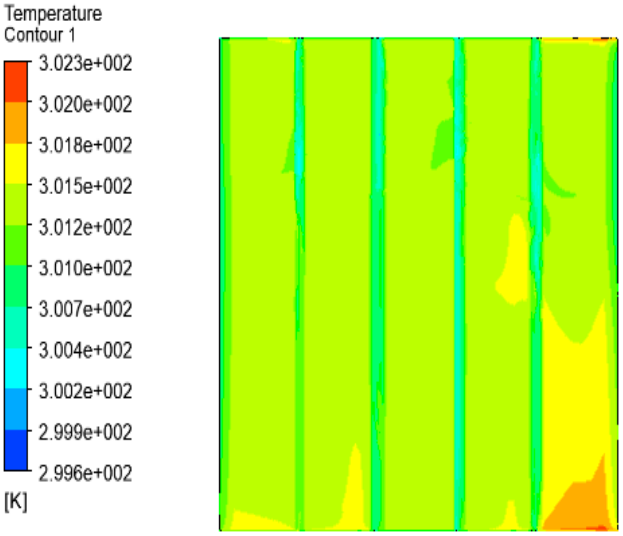

Smooth tube at Re= 10000

Fig. 5: Temperature contour

Effect of Turbulence Element on Outlet Temperature

Table 4.2 shows the fluid outlet temperature at different Reynolds numbers. According to this diagram, the base model has the lowest outlet temperature, whereas the Third model has the highest. In all cases, by increasing the Reynolds number, the chance of heat transfer between the fluid and the tube decreases, resulting in a lower outlet temperature. In addition, it is obvious that with increasing Reynolds number, the effect of different models on the output temperature will not be much different. Because increasing the Reynolds number and, of course, increasing the velocity does not create enough opportunity for the heat transfer of the structure and the fluid, so the difference between the outlet and inlet temperature will be very small.

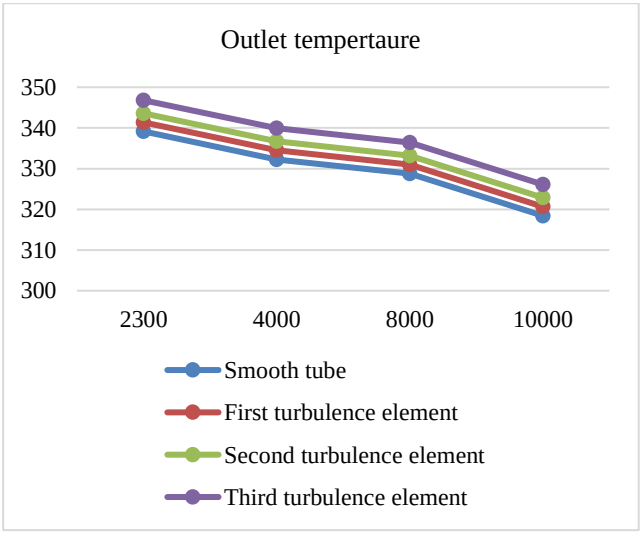

Fig. 6: Outlet temperature at different Reynolds number

Effect of Turbulence Element on Nusselt Number

Effect of turbulence element on Nusselt number is shown in Fig 4.8. The horizontal x-axis represents Reynolds number and y-axis represents Nusselt number. It is seen thatwith the addition of turbulence elementresults in increase in Nusselt number. Thismay be due to due to the secondary flows generated by turbulence-inducing elements, reducing the thickness of the thermal boundary layer and thus increasing the heat transfer rate. Moreover, the flow will be more turbulent with an increase in Reynolds number and cause a better heat transfer rate.

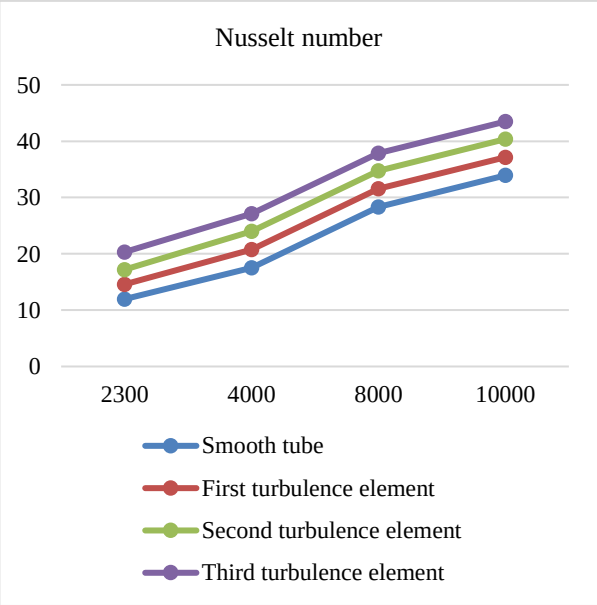

Fig.7: Variation of Nusselt at different Reynolds number

IV. CONCLUSION

1. Nusselt number increases whereas friction factor decreases with increase of Reynolds number. Values of friction factor and Nusselt number are higher as compared to those for smooth absorber plate. This is due to change in flow characteristics because of turbulence inducing that causes flow separation, reattachments and generation of secondary flow.
2. Rate of increase of Nusselt number with increasing Reynolds number is lower than rate of increase of friction factor because at higher values of turbulence inducing element height, reattachment of free shear layer does not occur and rate of heat transfer enhancement is not proportional to that of friction factor.
3. Maximum enhancement of Nusselt number and friction factor is observed at third turbulence inducing element.
4. Comparison of simulation values of Nusselt number andthose predicted by correlation lie within deviation range of 5%. It cantherefore be concluded that correlations for prediction ofNusselt number satisfactory.
5. For all the cases considered in this study, increase in Reynolds number leads to augmentation in Nusselt number.
6. Results showed that third case has a better heat transfer than the others
7. When turbulence inducing element are introduced just beneath the collector plate, there was a considerable alteration in the heat transfer coefficient of air.

REFERENCES

1. Agrawal, Y., Yugbodh, K., Ahmed, S. F., Jain, E., Bhagoria, J. L., Gautam, A., & Mishra, A. (2023). Experimental investigation of heat transfer and flow analysis of artificially roughened solar air heater by using double arc reverse shaped roughness with gap on the absorber plate. Materials Today: Proceedings, 78, 403-413.
2. Fadala, G. M., & Yousef, A. H. (2023). The effect of artificial roughness on performance of solar air heater (SAH): A review study. In AIP Conference Proceedings (Vol. 2776, No. 1, p. 050008). AIP Publishing LLC.
3. Chaurasia, S., Goel, V., &Debbarma, A. (2023). Impact of hybrid roughness geometry on heat transfer augmentation in solar air heater: A review. Solar Energy.
4. Saxena, R., Pachorkar, P., Jain, A., Majumder, H., Pandey, K. K., Mishra, S. K., &Kalbande, V. P. (2023). Performance enhancement of solar air heater using artificial roughness. Materials Today: Proceedings.
5. Yadav, A. K., Choudhary, M., & Singh, A. P. (2023). Assessment of solar air heater performance using a variety of artificially roughened components. Materials Today: Proceedings.
6. Singh, V. P., Jain, S., & Gupta, J. M. L. (2023). Analysis of the effect of perforation in multi-v rib artificial roughened single pass solar air heater:-Part A. Experimental Heat Transfer, 36(2), 163-182.
7. Kumar, D., &Layek, A. (2023). Heat Transfer Enhancement of Solar Air Heater Having Twisted V-Shaped Staggered Roughness Over Absorber Plate. Arabian Journal for Science and Engineering, 48(3), 3931-3946.
8. Arya, N., Goel, V., &Sunden, B. (2023). Solar air heater performance enhancement with differently shaped miniature combined with dimple shaped roughness: CFD and experimental analysis. Solar Energy, 250, 33-50.
9. Kumar, D., &Layek, A. (2022). Parametric analysis of artificial rib roughness for the enhancement of

thermohydraulic performance of solar air heater: A review. Materials Today: Proceedings, 57, 1127-1135.
10. Singh, H., Singh, H., & Kishore, C. (2022). CFD numerical investigation of Heat transfer characteristics of Y-shaped solar air heater. Materials Today: Proceedings, 52, 2003-2013.
11. Yadav, A. S., Gupta, S., Agrawal, A., Saxena, R., Agrawal, N., &Nashine, S. (2022). Performance enhancement of solar air heater by attaching artificial rib roughness on the absorber Plate. Materials Today: Proceedings, 63, 706-717.
12. Bhuvad, S. S., Azad, R., &Lanjewar, A. (2022). Thermal performance analysis of apex-up discrete arc ribs solar air heater-an experimental study. Renewable Energy, 185, 403-415.
13. Agrawal, Y., Bhagoria, J. L., Gautam, A., Sharma, A., Yadav, A. S., Alam, T., & Kumar, R. (2023). Investigation of thermal performance of a ribbed solar air heater for sustainable built environment. Sustainable Energy Technologies and Assessments, 57, 103288.
14. Alsaiari, A. O., Iqbal, A., Abdulkhair, H., Gzara, L., Almatrafi, E., Alzahrani, H. A., ... &Aljohani, M. (2022). Heat transmission and air flow friction in a solar air heater with a ribbed absorber plate: A computational study. Case Studies in Thermal Engineering, 40, 102517.
15. Agrawal, Y., &Bhagoria, J. L. (2021). Experimental investigation for pitch and angle of arc effect of discrete artificial roughness on Nusselt number and fluid flow characteristics of a solar air heater. Materials Today: Proceedings, 46, 5506-5511.